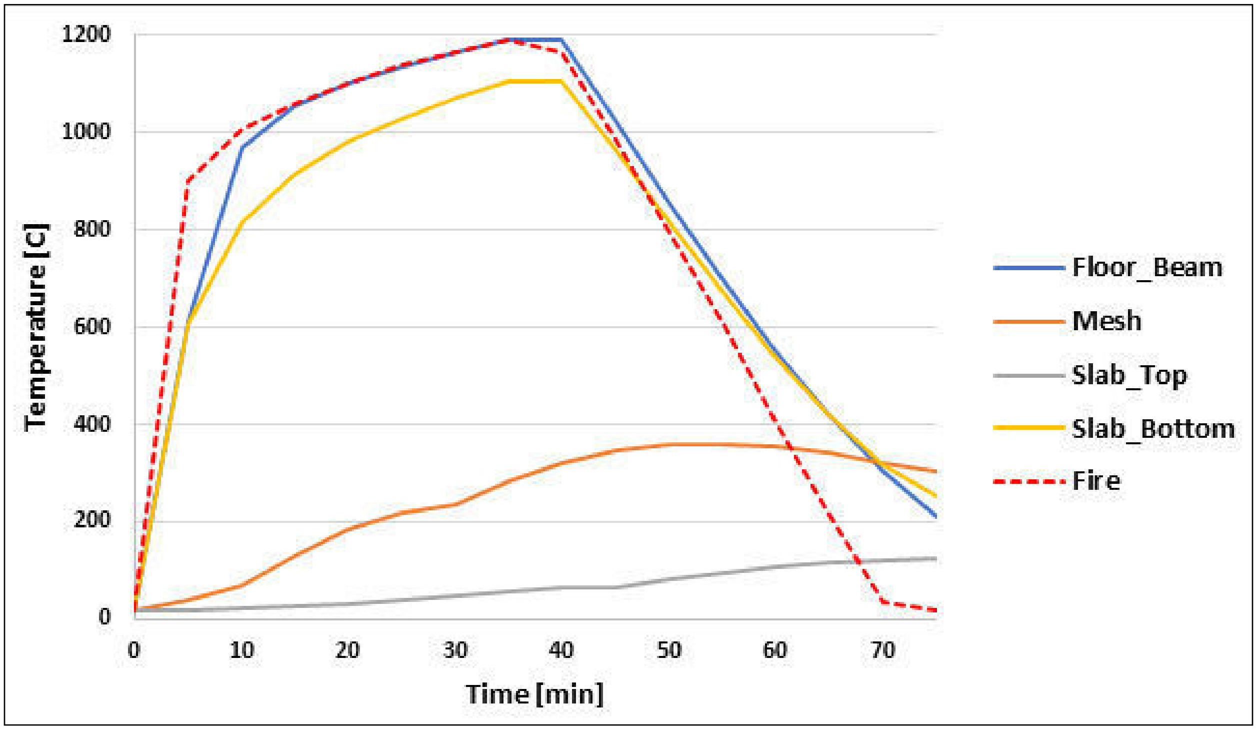

Figure 7-15. Structural temperature histories during fire exposure (Case 10).
Source: Courtesy of Simpson Gumpertz & Heger (2019).

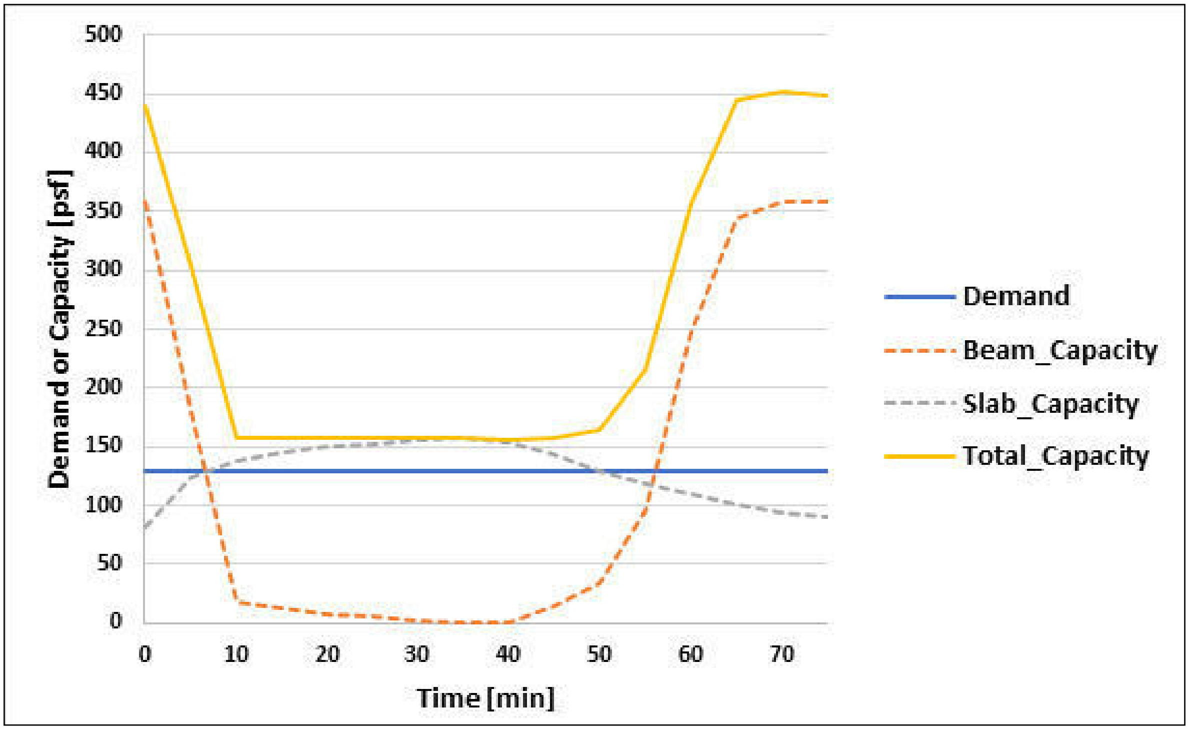

Figure 7-16. Floor demand/capacity history during fire exposure (Case 10).
Source: Courtesy of Simpson Gumpertz & Heger (2019).

Table 7-2. Atypical Floor Systems Analyzed.

Config-uration	Bay Width	Bay Length	Infill Beams	Bound-ary Beam 1	Bound-ary Beam 2	Girder 1	Girder 2	Controlling Periphery Member Temperature
Base	30 ft	30 ft	W16x26	W16x26	W16x26	W24x55	W24x55	597 °C
2	30 ft	30 ft	W16x26	W16x26	W16x26	W24x55	W18x35	597 °C
3	30 ft	30 ft	W16x26	W16x26	W18x35	W24x55	W18x35	597 °C
4	30 ft	30 ft	W16x26	W16x26	W16x26	W21x50	W18x35	597 °C
5	30 ft	30 ft	W16x26	W16x26	W16x26	W21x44	W24x55	597 °C
6	30 ft	30 ft	W16x26	W16x26	W24x62	W21x50	W24x55	597 °C
7	30 ft	30 ft	W18x35	W18x35	W18x35	W18x35	W24x55	656 °C
8	30 ft	30 ft	W18x35	W18x35	W18x35	W24x55	W24x55	656 °C
9	30 ft	30 ft	W18x35	W18x35	W18x35	W21x44	W24x55	656 °C
10	30 ft	30 ft	W18x35	W24x68	W24x68	W21x44	W24x55	700 °C
11	30 ft	30 ft	W18x35	W18x35	W24x62	W24x55	W24x55	656 °C
12	30 ft	30 ft	W16x26	W16x26	W24x62	W18x35	W21x50	597 °C
13	30 ft	30 ft	W18x35	W18x35	W24x62	W18x35	W24x55	656 °C
14	30 ft	18 ft	W16x26 (1)	W18x35	W16x31	W40x167	W40x183	695 °C
15	30 ft	18 ft	W16x26 (1)	W18x35	W16x26	W33x130	W40x183	677 °C
16	30 ft	18 ft	W16x26 (1)	W16x26	W16x31	W18x35	W18x35	677 °C
17	30 ft	18 ft	W16x26 (1)	W16x26	W16x26	W18x35	W18x35	677 °C
18	30 ft	18 ft	W18x35 (1)	W18x35	W18x35	W18x35	W18x35	725 °C
19	30 ft	18 ft	W18x35 (1)	W24x55	W24x68	W18x35	W18x35	809 °C

Even considering inconceivably low ventilation cases (as low as approximately 300 sq. ft of total ventilation area from the fire zone) for the *above-design* fuel load, the floor system still survives full burnout, and survives at least 130 min when the absolute lower bound ventilation opening factor of 0.02 is considered. Also, the floor system would survive approximately 70 min under the 3X-design fuel load case with low ventilation, which upholds the minimum performance expectation (as discussed in Section 2.3.1) under a nearly inconceivable fuel load level. Overall, the variety of conditions in which the floor system performs adequately demonstrates the reliability/robustness of the enhanced floor design, which was not possible to achieve for Designs 1 and 2.

To corroborate the Design 3 structural analyses conducted using MACS+/SPM and to extract connection force histories (see Section 7.6.5), SAFIR was used to simulate a single structural bay for the *above-design* fuel load with low ventilation case for a 4 h time frame to capture the entirety of the cooling phase (Figure 7-17). In this model, the periphery members are pin-released, using the software's *SAME* function to ensure that they undergo the maximum possible deflection, which is conservative. In addition, the axial stiffness of the girder/boundary beam–column connections are represented in the model using the software's *RELAX* function. Hand calculations were conducted to determine the axial stiffness of the girder/boundary beam–column connections, and these values were conservatively taken at ambient, which would produce the highest level of restraint.

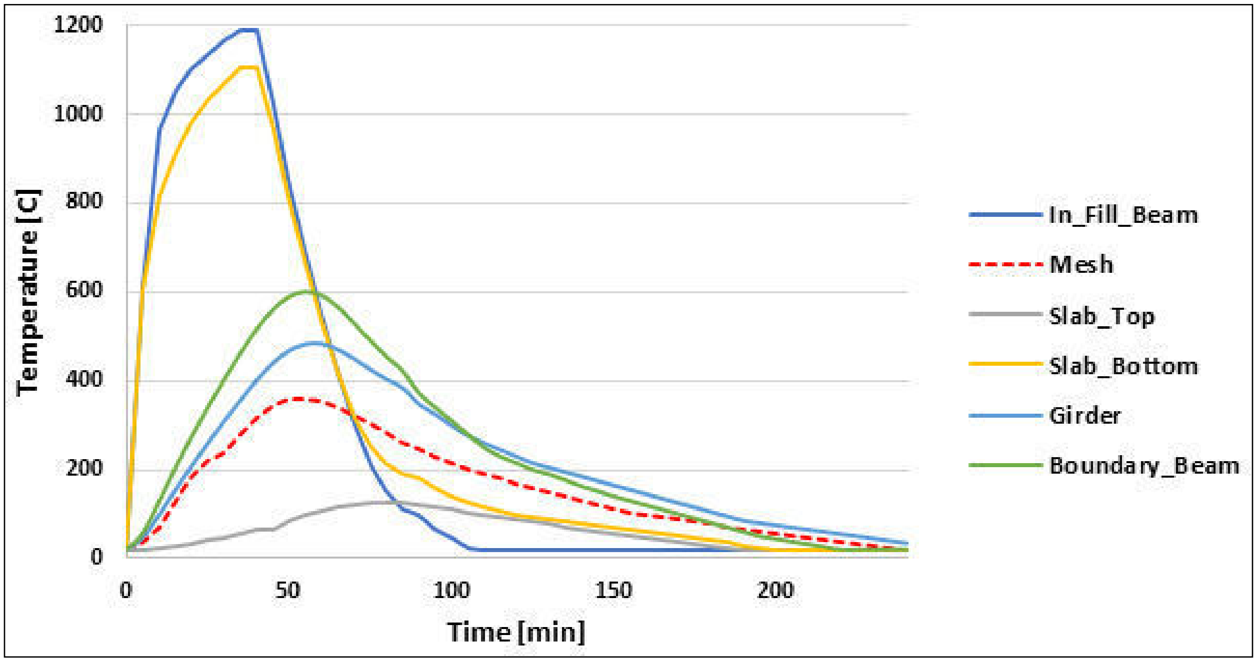

Figure 7-17. Structural temperature histories (Case 10 extended to 4 h).

Source: Courtesy of Simpson Gumpertz & Heger (2019).

The single-bay SAFIR model survives full burnout without any instability (including any mesh yielding), which corroborates the previous results. Figure 7-18 plots the deflection histories of the floor members. Figures 7-19 and 7-20 illustrate the evolution of the floor slab deflection and principal membrane forces as it heats and cools, respectively. A case in which 25% of the floor loading from adjacent bays (also under fire exposure) is shed to the single (modeled) bay (approximately 1 kip/ft added to the periphery members) was simulated, and no floor failure was observed. This case would also account for any cladding load at the edges of the building (approximately 0.2 kip/ft). Also, the floor system was simulated without thermal expansion represented to confirm that stable tensile membrane action could form without restraint effects (i.e., owing to deflection compatibility alone).

To corroborate the performance of the single-bay SAFIR model, multi-bay scenarios were considered. As an upper bound restraint condition, in-plane rigid restraints were applied to the full periphery of the slab (single-bay model), and no floor failure were observed. Also, explicit representation of various slab restraint conditions was simulated with a nine-bay SAFIR model with fire exposing an interior bay, an edge bay, and a corner bay as illustrated in Figure 7-21. Figure 7-22 shows floor member deflections for the interior bay fire condition. As expected, these simulated conditions demonstrate no floor failure, as shown in Figures 7-23 through 7-31.

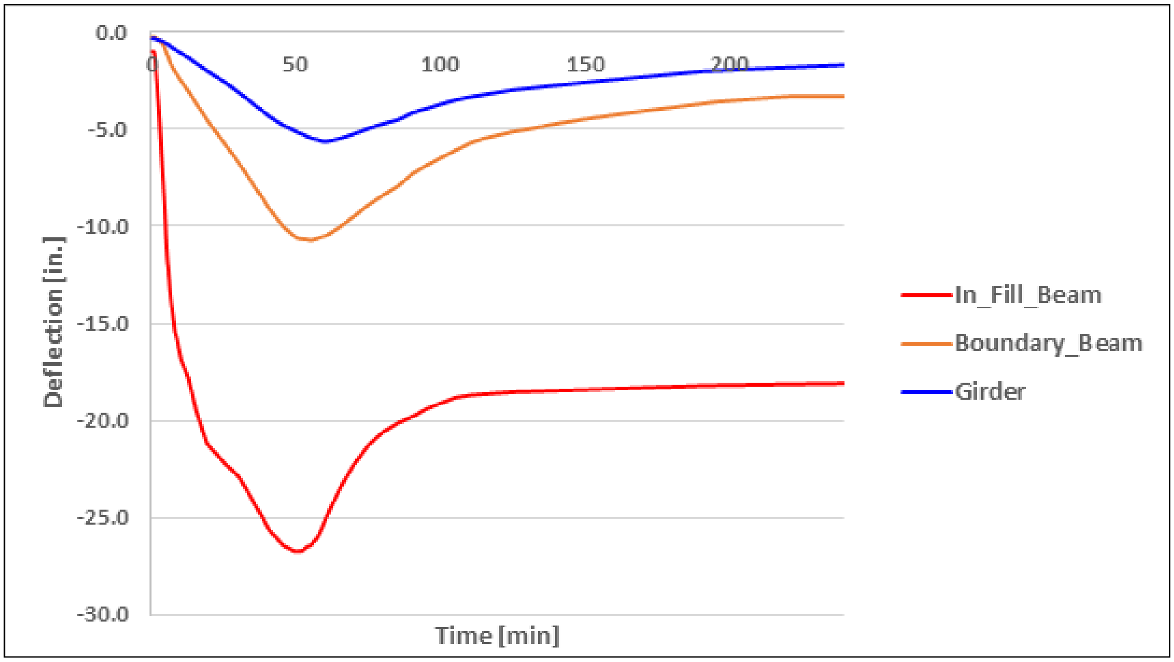

Figure 7-18. Floor member deflection histories (Case 10).
Source: Courtesy of Simpson Gumpertz & Heger (2019).

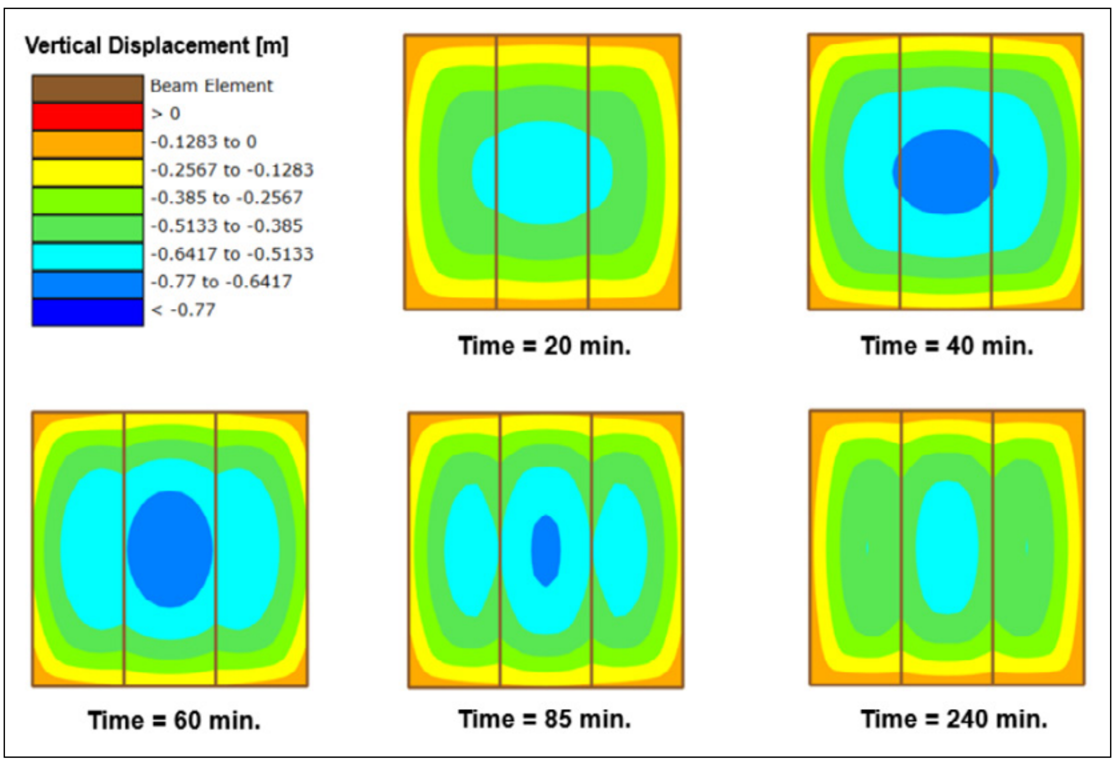

Figure 7-19. Floor slab deflection (Case 10).
Source: Courtesy of Simpson Gumpertz & Heger (2019), and SAFIR Software ©2019.

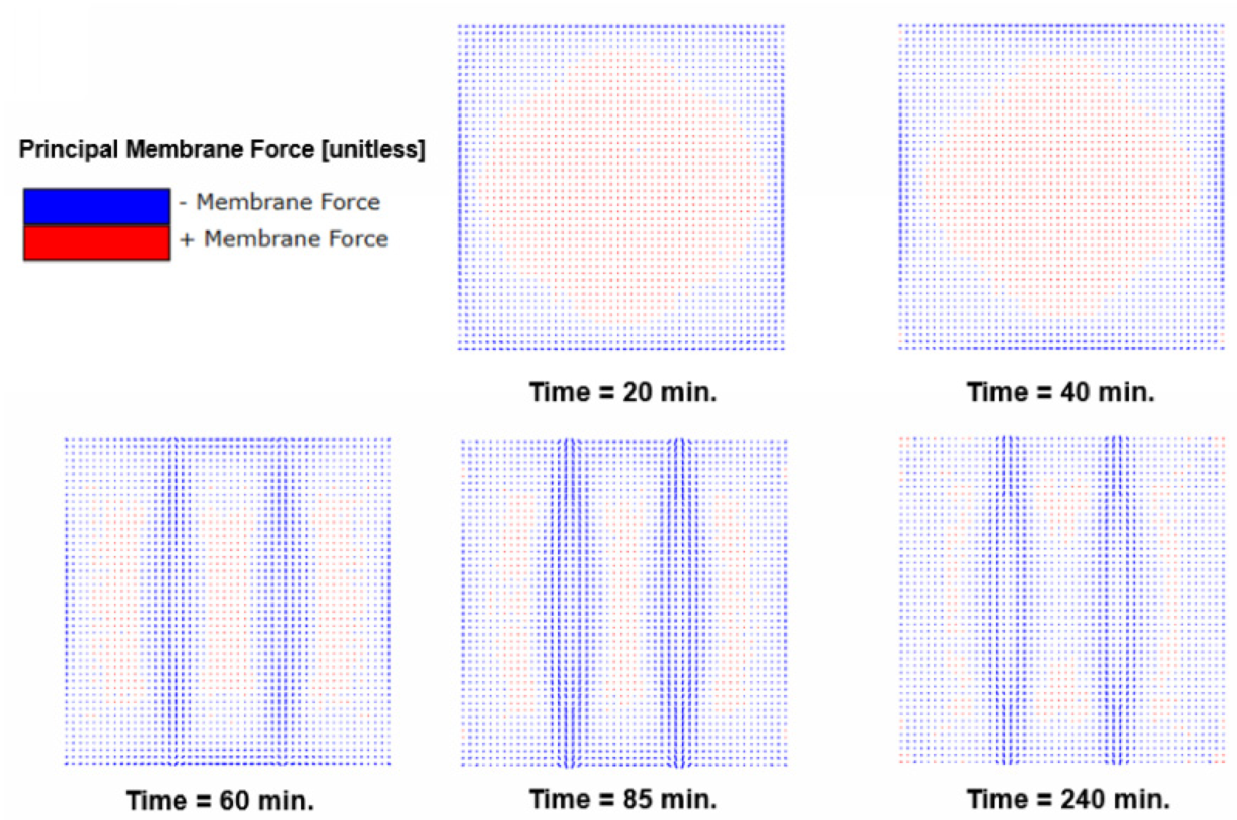

Figure 7-20. Floor slab principal membrane forces (Case 10).
Source: Courtesy of Simpson Gumpertz & Heger (2019), and SAFIR Software ©2019.

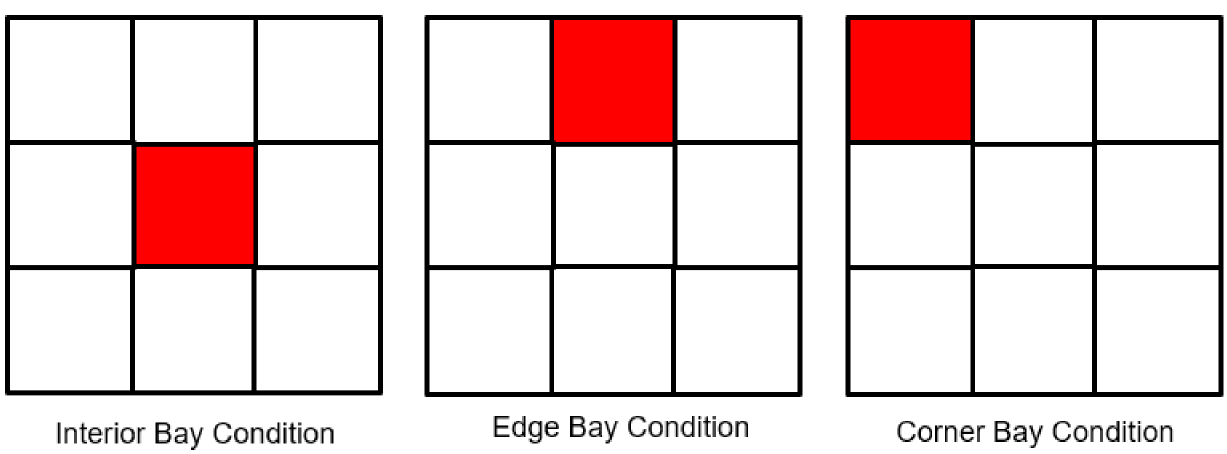

Figure 7.21. Fire locations (sensitivity studies of floor bay restraint).
Source: Courtesy of Simpson Gumpertz & Heger (2019).

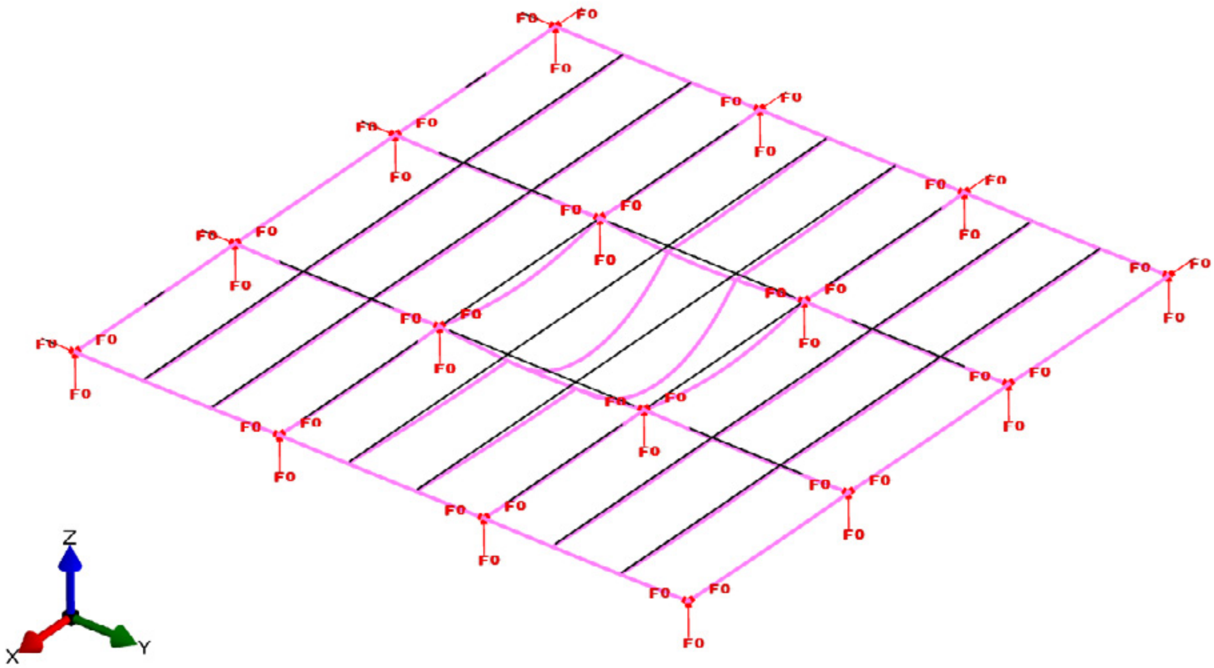

Figure 7-22. Floor member deflection for interior bay fire condition.
Source: Courtesy of Simpson Gumpertz & Heger (2019), and SAFIR Software ©2019.

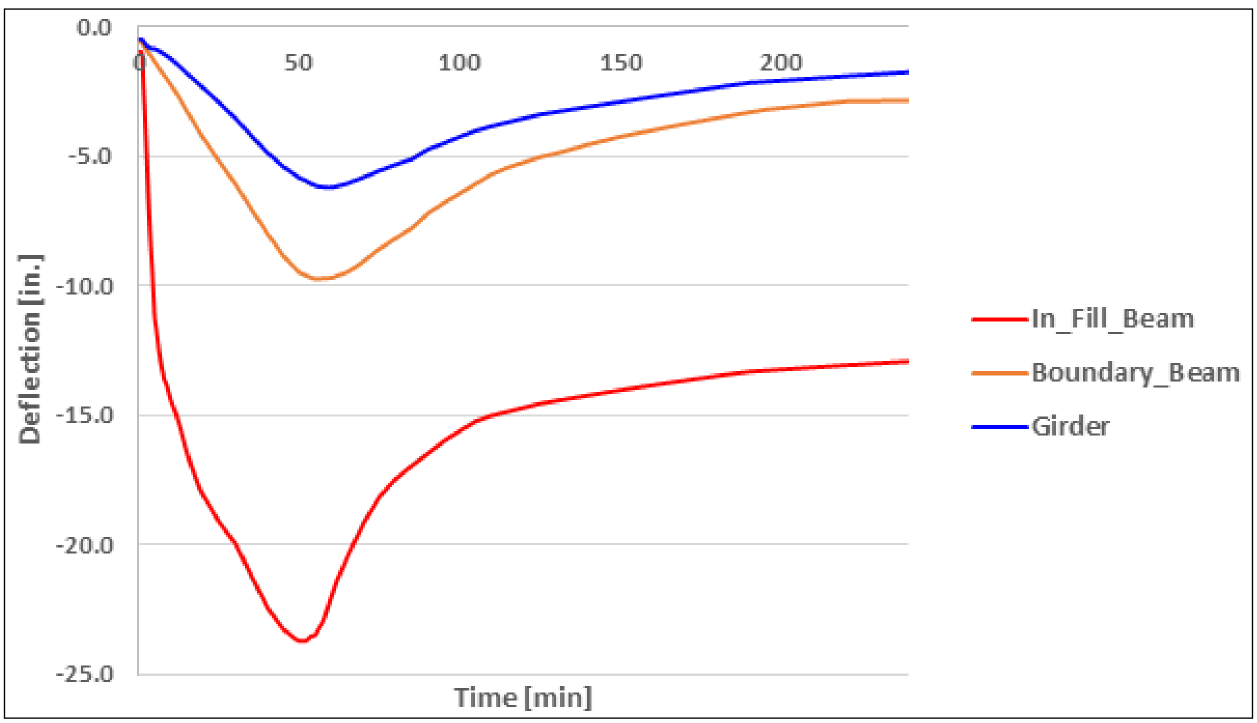

Figure 7-23. Floor member deflection histories (Case 10) (interior bay fire).
Source: Courtesy of Simpson Gumpertz & Heger (2019).

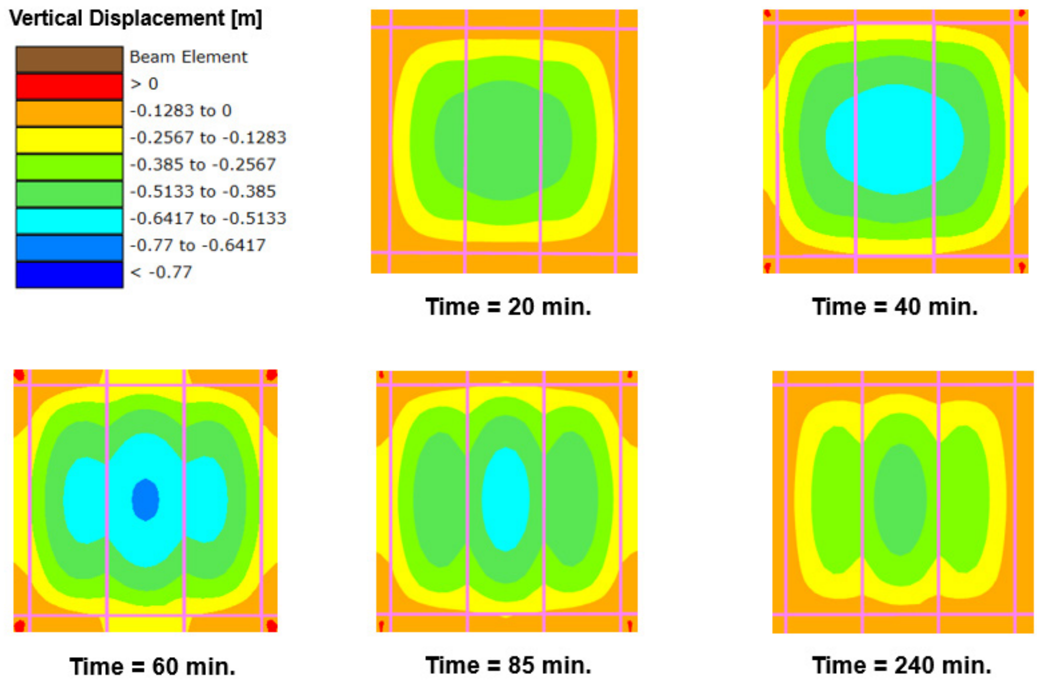

Figure 7-24. Floor slab deflection (Case 10) (interior bay fire).
Source: Courtesy of Simpson Gumpertz & Heger (2019), and SAFIR Software ©2019.

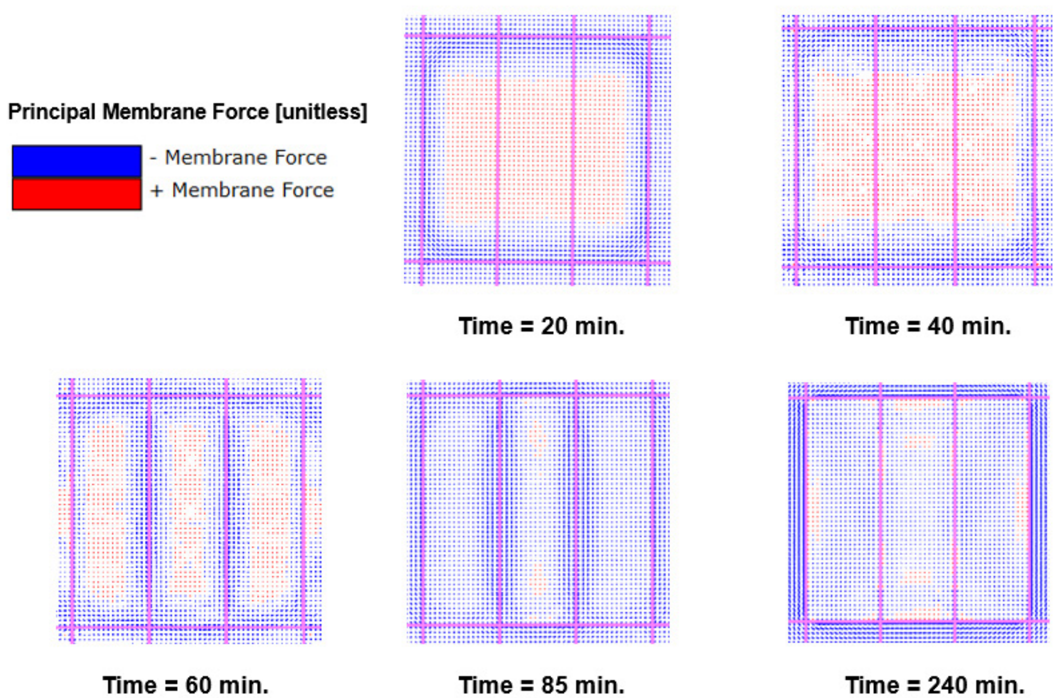

Figure 7-25. Floor slab principal membrane forces (Case 10) (interior bay fire).
Source: Courtesy of Simpson Gumpertz & Heger (2019), and SAFIR Software ©2019.

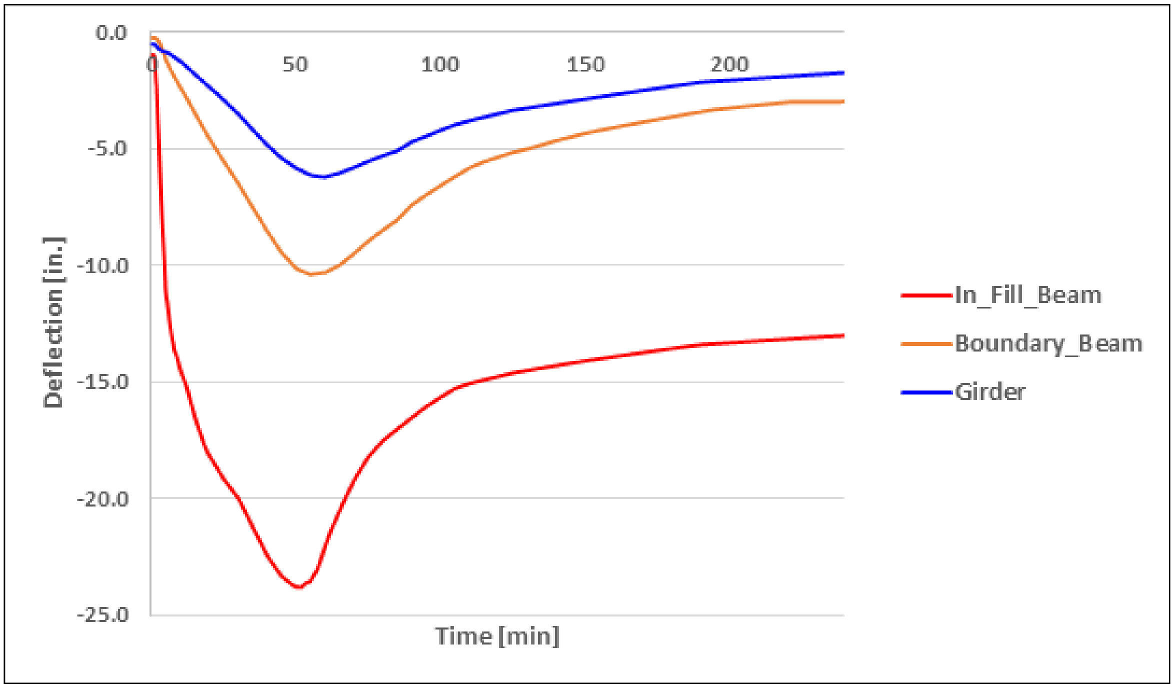

Figure 7-26. Floor member deflection histories (Case 10) (edge bay fire).
Source: Courtesy of Simpson Gumpertz & Heger (2019).

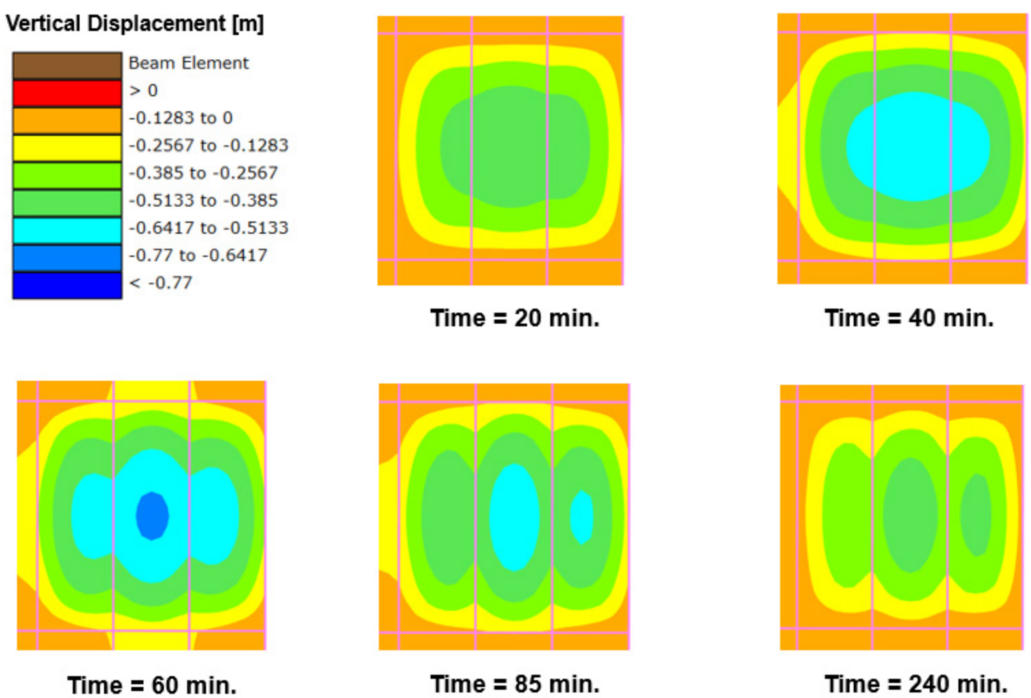

Figure 7-27. Floor slab deflection (Case 10) (edge bay fire).
Source: Courtesy of Simpson Gumpertz & Heger (2019), and SAFIR Software ©2019.

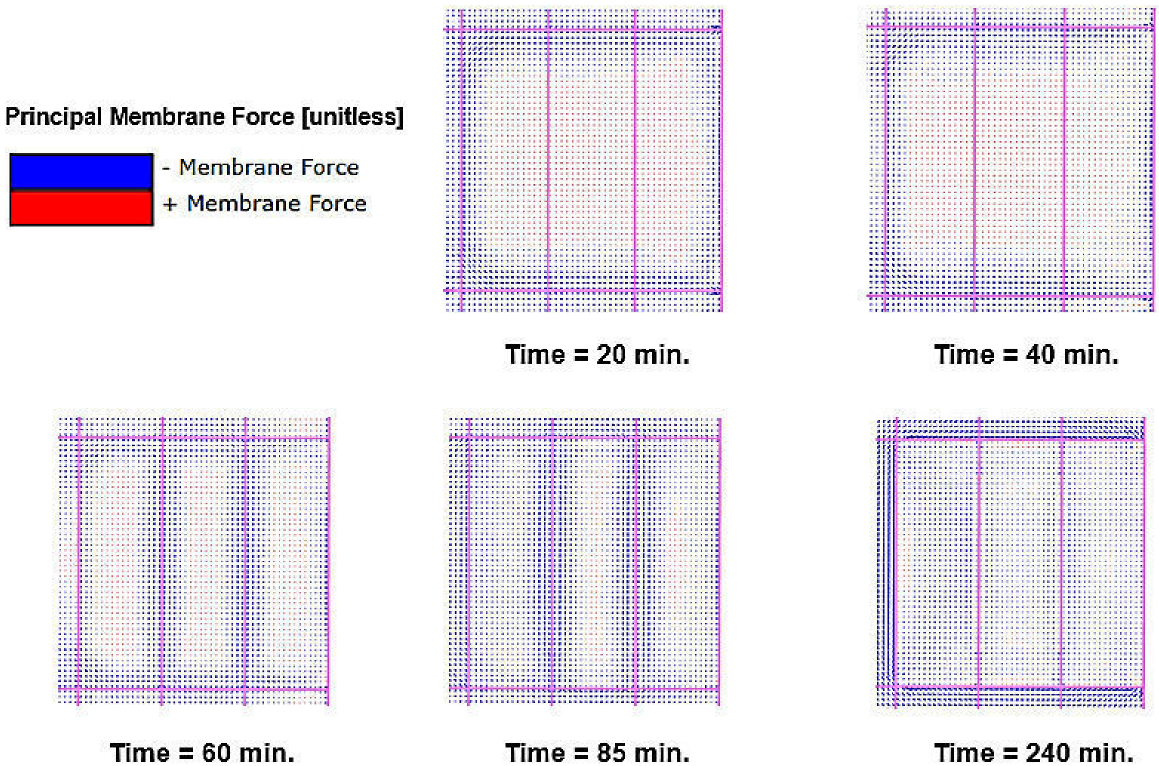

Figure 7-28. Floor slab principal membrane forces (Case 10) (edge bay fire).
Source: Courtesy of Simpson Gumpertz & Heger (2019), and SAFIR Software ©2019.

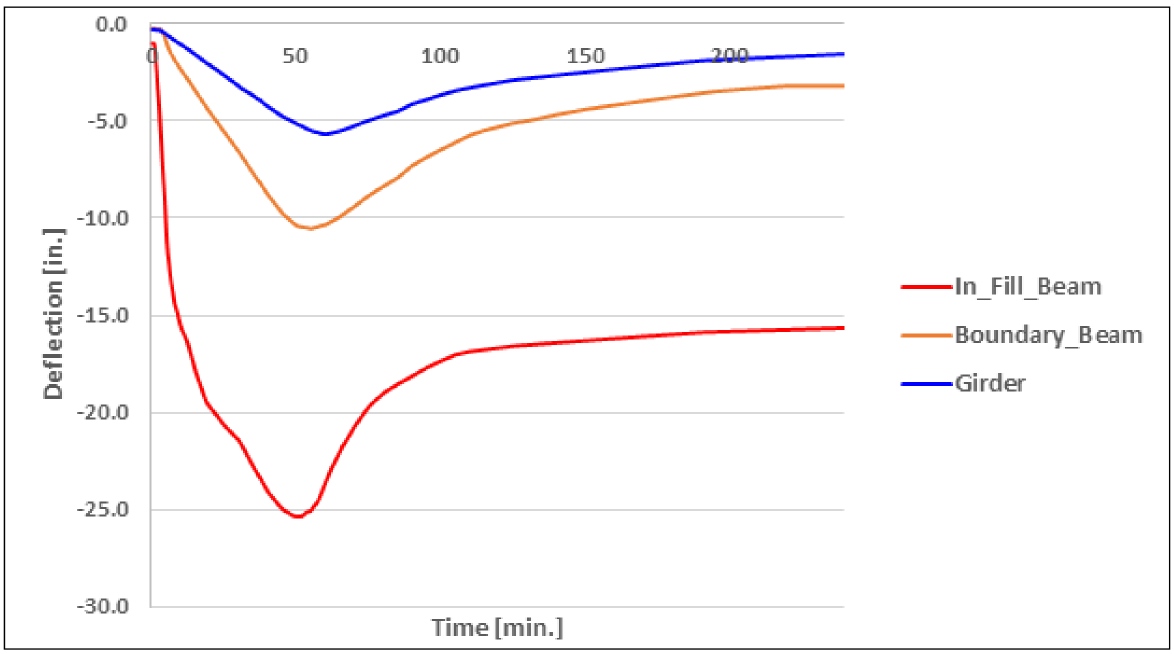

Figure 7-29. Floor member deflection histories (Case 10) (corner bay fire).
Source: Courtesy of Simpson Gumpertz & Heger (2019).

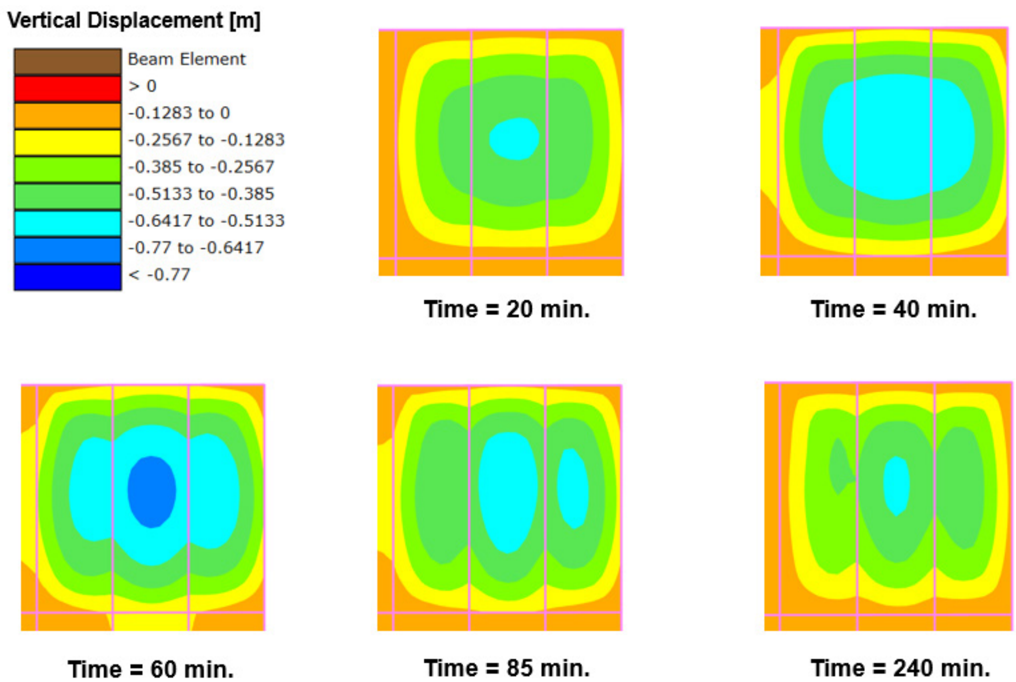

Figure 7-30. Floor slab deflection (Case 10) (corner bay fire).
Source: Courtesy of Simpson Gumpertz & Heger (2019), and SAFIR Software ©2019.

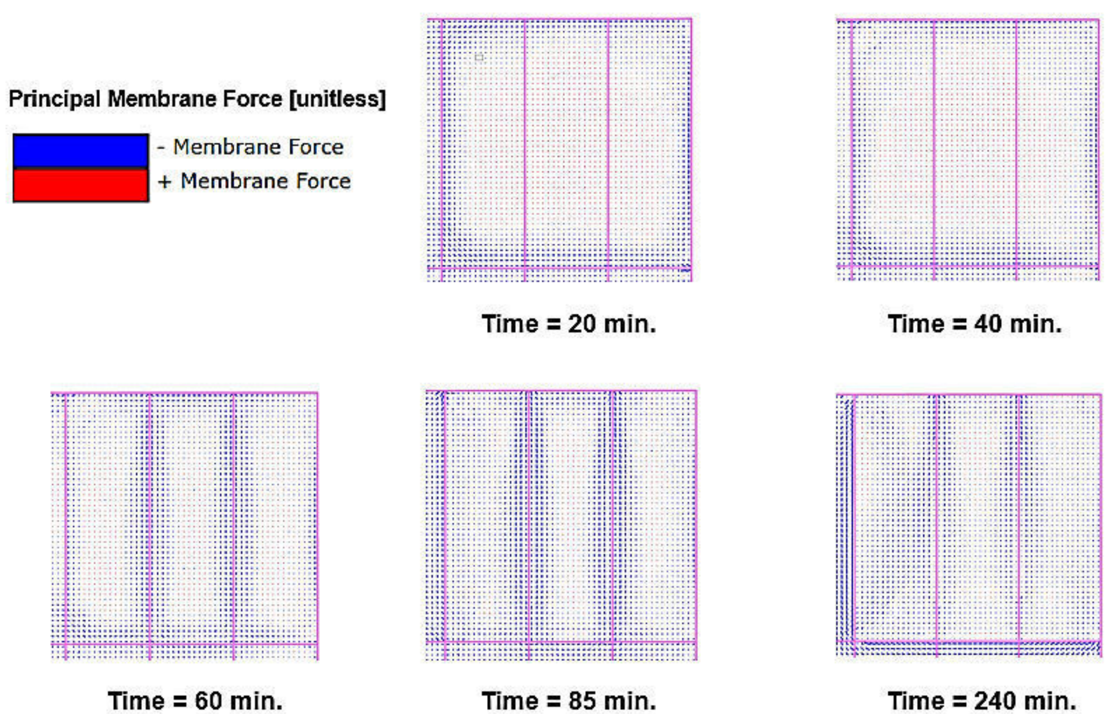

Figure 7-31. Floor slab principal membrane forces (Case 10) (corner bay fire).
Source: Courtesy of Simpson Gumpertz & Heger (2019), and SAFIR Software ©2019.